Anisotropic field ionization in nanoclusters mediated by a Brunel-electron-driven plasma wave

Xiaohui Gao *

Department of Physics, Shaoxing University, Shaoxing, Zhejiang 312000, China

(Received 19 May 2023; accepted 11 September 2023; published 22 September 2023)

Ionization is one of the most fundamental processes in intense laser-matter interaction. It is extremely efficient for clusters in laser fields and often leads to surprisingly high charge states at moderate laser intensities. Here we show an interesting ionization mechanism in laser-cluster interaction through particle-in-cell simulations. As the laser field ionizes a cluster, Brunel electrons pushed back into the clustered plasma form attosecond bunches, impulsively exciting plasma oscillation. The resulting localized wake field further ionizes the cluster, causing a highly ionized rodlike core along the polarization axis. This anisotropic ionization is prominent using few-cycle pulses and may be washed out using longer pulses due to collisional ionization. This unexpected ionization channel can potentially provide complicated site-specific control of high ionization in nanometer-scale targets.

DOI: 10.1103/PhysRevA.108.033109

I. INTRODUCTION

Laser-cluster interaction has been a subject of strong scientific interest for several decades [1–3]. The localized high density in connection with the isolated environment enables efficient laser-matter coupling, providing not only a unique platform for studying the ultrafast nonequilibrium dynamics [2] but also various practical applications ranging from particle accelerators [4,5] to neutron sources [6] and nuclear isomer sources [7].

A fascinating aspect of intense laser-cluster interaction is the surprisingly efficient ionization and heating. A deep understanding of the ionization dynamics is of intrinsic interest to the high-field physics community, and finding a convenient way to control this process is of practical relevance for applications such as particle acceleration by Coulomb explosion. As the first step in intense laser-cluster interaction, ionization has been investigated extensively. It is generally divided into two categories, i.e., field ionization and collisional ionization. Efficient field ionization in clusters is often due to field enhancement, which may originate from field resonance at the critical density [8,9] or field amplification due to cluster polarization [10]. The ionizing electric field is not limited to the laser field and can be the electric field due to charge separation, such as hot electron bunches [11] or the free plasmon oscillations of clustered plasma driven by few-cycle pulses [12,13], and the sheath electric field generated by a hot electron population in a clustering gas jet [14]. Collisional ionization by energetic electrons is another important contribution for the high ionization in clusters [15], but it favors longer pulses and plays a minor role for extremely short pulses [16]. The contribution of different ionization channel depends on the laser parameters and cluster properties such as the wavelength and the size [17,18], and the physical picture may not yet be exhaustive.

While many interesting phenomena of laser-cluster interaction stem from the resonant behavior of the electrons confined within the cluster, the role of Brunel electrons is less explored. Some electrons near the surface may be pulled out of the cluster and pushed back into the plasma as the laser field decreases. These electrons, known as Brunel electrons, are responsible for the efficient heating in clusters [19,20]. Brunel electrons are well studied in laser interaction with solid-density bulk plasmas, uncovering a multitude of intriguing phenomena such as vacuum heating [21] and coherent wake emission [22,23].

In this paper, we study the ionization dynamics of rare-gas clusters in ultrashort near-infrared laser pulses at moderate intensities via particle-in-cell simulations. Under the irradiation of few-cycle pulses, the charge state distribution is highly nonuniform and exhibits a pronounced rodlike hot region along the polarization axis. This enhanced ionization is due to the electric field of plasma oscillation driven by Brunel-electron bunches, similar to the process in the overdense plasmas giving rise to coherent wake emission. We also find that collisional ionization is detrimental to this exotic charge distribution, and the hot spot at the center disappears with longer pulses.

II. SIMULATION SETTINGS

Our simulations are performed using the open-source three-dimensional particle-in-cell code SMILEI [24]. The dimensions of the simulation box are $6\lambda \times 0.4\lambda \times 0.4\lambda$, where λ is the wavelength. The grid resolution is 320 cells per wavelength, and the time resolution is 580 steps per cycle. A cluster sits at the center of the simulation box with 125 un-ionized macroparticles in each cell. The laser pulse enters

*gaoxh@utexas.edu

the simulation box along the x axis from the left. The pulse is linearly polarized in the y direction and is assumed to be a plane wave in space and a Gaussian profile in time. The field employs Silver-Müller boundary conditions for the longitudinal direction and periodic boundary conditions for the transverse directions. Field ionization, electron-electron collision, electron-ion collision, and collisional ionization are included in the simulation using standard modules of the code. Recombination is not accounted for, which should not alter the dynamics significantly in the few-cycle regime. The polarizability of the neutral atom is neglected, which is justified when the size is much smaller than the wavelength or the intensity is substantially higher than the ionization threshold [25]. In all of our simulations, we consider a spherical argon cluster interacting with an 800 nm pulse. The cluster radius is 40 nm, which is large enough to capture the dynamics due to the plasma wave as the size is several times the plasma oscillation wavelength. Such clusters are routinely produced in experiments by pulsed gas jets backed with high-pressure gases. The atomic density of the argon cluster is 2.6×10^{22} cm^{-3} [26], which corresponds to $15n_c$, with n_c being the critical density at 800 nm.

III. RESULTS AND DISCUSSION

Figure 1 shows snapshots of the interaction of a 40-nm argon cluster with an intense ultrashort pulse at different observation times. The peak intensity is 5.0×10^{15} W/cm^2, and the full width at half maximum (FWHM) of the field is two-cycle with zero carrier-envelope phase. Figures 1(a) and 1(b) present the charge state distribution in the x-y plane and x-z plane, respectively, at a time of observation $t = 10.02$ fs, at which time the pulse has already passed the cluster. An enhanced ionization is observed at the cluster center with a rodlike hot region orientated along the polarization axis. This is in sharp contrast with a general perception that ionization occurs preferentially at the periphery of the cluster due to the skin effect. The skin depth for a plasma in a laser at a nonresonant wavelength is $\delta \approx c/\omega_p$, where c is the speed of light in a vacuum and ω_p is the plasma frequency. This corresponds to $\delta \approx 19$ nm for an average charge state of 3. The formation dynamics of this unexpected ionization pattern is illustrated in Figs. 1(c)–1(f). The initial ionization is due to the propagation of the laser field and is higher in the front surface. An ionization wave, however, propagates from the bottom pole toward the center, as shown in the snapshot of the charge state distribution at $t = 0.09$ fs in Fig. 1(c). The snapshot of the charge state distribution at $t = 0.74$ fs in Fig. 1(d) shows another ionization wave propagating from the top pole toward the center. The ionization is consistent with the corresponding field distribution E_y shown in Figs. 1(e) and 1(f).

To clarify the underlying ionization mechanism, streaks of the electron density n_e, transverse field E_y, and charge state Z_{Ar} along the polarization axis are presented against the observation time. Figure 2(a) shows that a small fraction of electrons are pulled into vacuum by the laser field and are then sent back into the cluster. This occurs alternatingly at the top pole and at the bottom pole every half cycle. As Brunel electrons with a longer trajectory gain more energy than those with a shorter trajectory, trajectory crossing occurs inside the

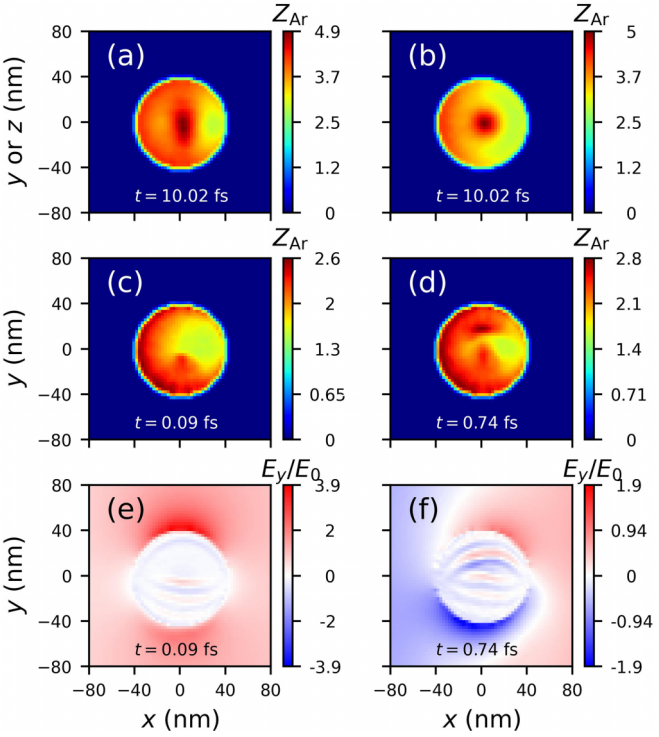

FIG. 1. Snapshots of an argon cluster subject to a two-cycle (FWHM in field) 800 nm pulse. (a) and (b) show the charge state distribution in the y-x plane and in the z-x plane, respectively, at $t = 10.02$ fs. (c) and (d) show the charge state distribution in the y-x plane at $t = 0.09$ fs and $t = 0.74$ fs, respectively. (e) and (f) show the transverse field E_y in the y-x plane at $t = 0.09$ fs and $t = 0.74$ fs, respectively. The electric field is normalized by the driving laser field E_0, and $t = 0$ marks the time at which the peak of the pulse reaches $x = 0$.

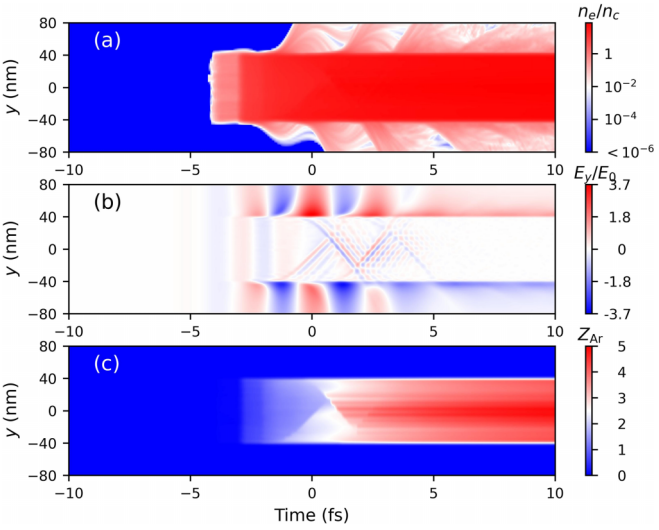

FIG. 2. Time evolution of three quantities at the polarization axis $(x, z) = (0, 0)$. (a) Electron density n_e normalized by the critical density n_c. (b) Transverse field E_y normalized by the driving field E_0. (c) Charge state Z of the argon atoms.

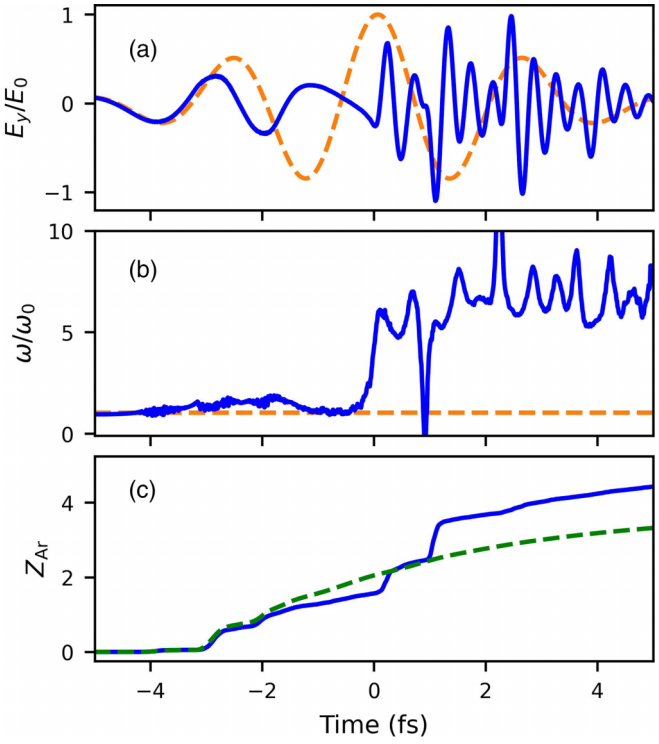

FIG. 3. (a) Normalized electric field E_y/E_0 at the center of the cluster as a function of time. (b) The corresponding instantaneous angular frequency ω normalized by the laser angular frequency ω_0. The dashed orange curves show the case when a cluster is not present. (c) Charge state Z at the center (solid blue curve) and charge state averaged over the entire cluster (dashed green curve) as a function of time.

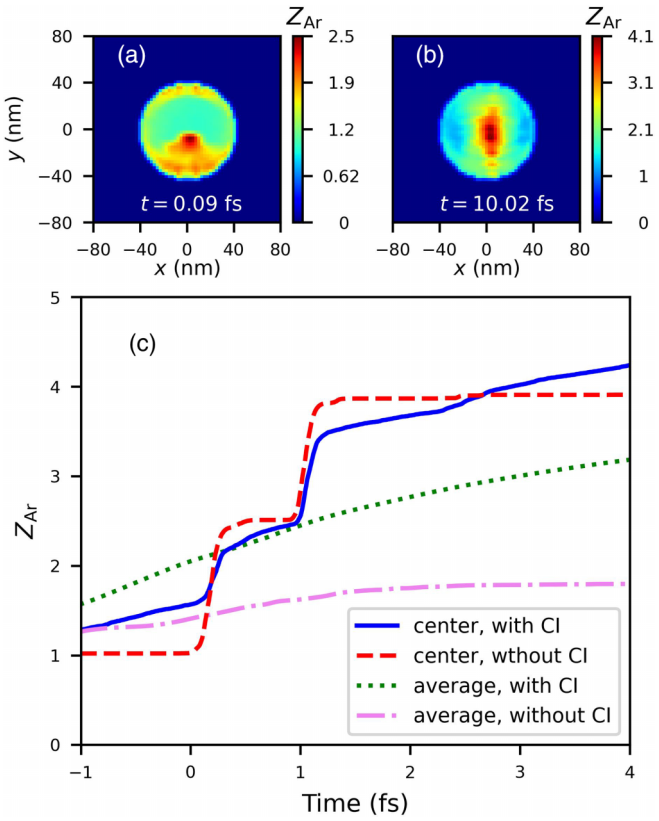

FIG. 4. Charge state distribution in the y-x plane at two observation times, (a) $t = 0.09$ fs and (b) $t = 10.02$ fs. (c) Time evolution of the charge state at the center of the cluster and the charge state averaged over the entire cluster with and without collisional ionization (CI).

cluster, and an attosecond electron bunch is formed with an appreciable electron density peak, exciting collective plasma oscillations of frequency ω_p in its wake. The analysis of the plasma oscillation excited by Brunel electrons is similar to the process in plasma mirrors [22,23] except for two distinct features. First, the plasma wave in clusters has a curvature due to the spherical geometry, leading to an increased oscillation amplitude as the wave converges. Secondly, the waves are excited twice in every cycle in clusters as Brunel electrons are produced in both the top and bottom parts of the clusters. The evolution of the plasma wave can be seen from Fig. 2(b), where the plasma oscillations are damped quickly, and oscillations excited from different bunches have interference. The ionization front shown in Fig. 2(c) occurs at the same time of the plasma wave, confirming that the Brunel-electron-driven plasma wave is responsible for the enhanced ionization at the core of clusters.

Figures 3(a) and 3(b) show the temporal electric field $E_y(t)$ and the corresponding instantaneous angular frequency $\omega(t)$, respectively, calculated as the temporal derivative of the oscillation phase of the electric field at the cluster center. Figure 3(c) shows the time evolution of the charge state at the cluster center (solid blue curve) and the charge state averaged over the entire cluster (dashed green curve). The field is initially shielded due to ionization at the surface. At approximately $t = 0$, the field starts to oscillate at roughly six times that of the laser frequency, and the charge state at the center rises steeply. This corresponds to the time that the first electron bunch travels to the cluster center. Note that the electron density is approximately $30n_c$. Thus the field oscillates roughly at ω_p rather than the surface plasmon frequency $\omega_p/\sqrt{3}$. The charge state exhibits a second steep rise approximately at $t = 0.9$ fs, at which time the instantaneous frequency exhibits a sharp dip. This is caused by the interference of plasma oscillations excited by the electron bunch entered from the bottom pole and that from the top pole. After $t = 0.9$ fs, the charge state at the cluster center is substantially higher than the average charge state, indicating the formation of a highly ionized core.

Collisional ionization is the other ionization channel when a fast electron bunch travels in a partially ionized plasma. To evaluate its role, collisional ionization is switched off, and the resulting charge distribution at two observation times, $t = 0.09$ fs and $t = 10.02$ fs, is shown in Figs. 4(a) and 4(b), respectively. With field ionization alone, an even more pronounced anisotropic ionization is observed. The temporal variations of Z_{Ar} at the center and Z_{Ar} averaged over the entire cluster for cases with and without collisional ionization are presented in Fig. 4(c). In spite of the few-cycle pulse duration, collisional ionization significantly increases the average charge and causes further ionization when the pulse is gone ($t > 2$ fs). Interestingly, the collisional ionization brings the

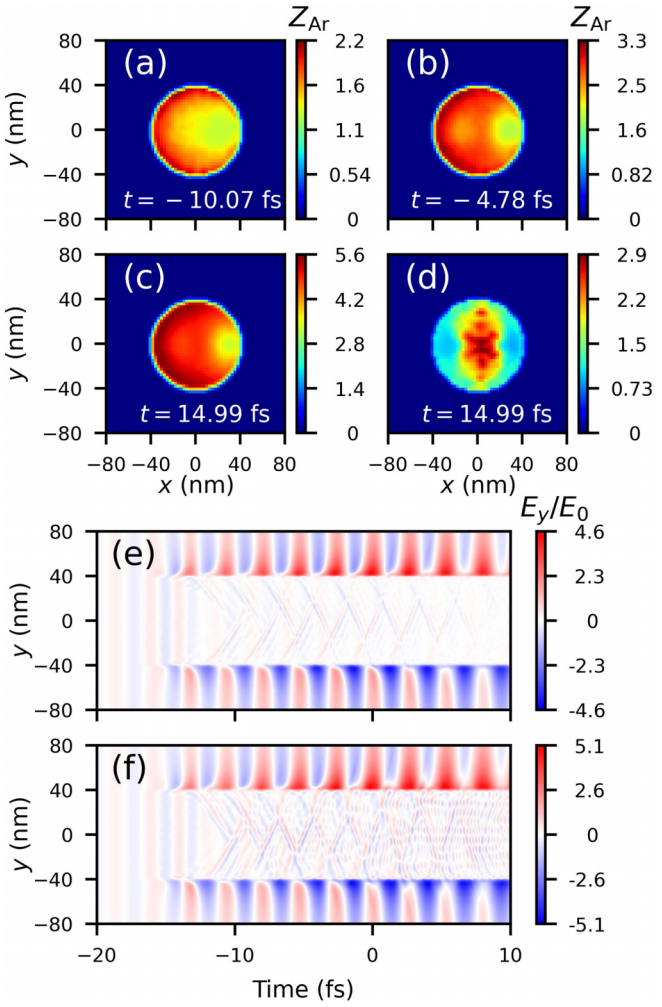

FIG. 5. Results of a 40-nm argon cluster interacting with a ten-cycle (FWHM in field) pulse of 2.0×10^{15} W/cm^2. Charge state distribution in the y-x plane at three observation times: (a) $t = -10.07$ fs, (b) $t = -4.78$ fs, and (c) $t = 14.99$ fs. (d) Charge state distribution in the y-x plane at $t = 14.99$ fs when collisional ionization is switched off. (e) Time evolution of transverse field E_y at polarization axis $(x, z) = (0, 0)$. (f) The case when collisional ionization is switched off.

charge state at the center slightly down between $t = 0$ and $t = 2$ fs. The reason for this could be that the collisional ionization dissipates the energy of driving electron bunches, leaving an inefficient excitation of the plasma oscillation.

Because of the negative role of the collisional ionization in the plasma oscillation, it is expected that enhanced core ionization may disappear at longer pulses. This is confirmed in the simulation for a ten-cycle pulse at 2.0×10^{15} W/cm^2 peak intensity. Figure 5(a) shows that ionization starts at the front surface of the cluster, and Fig. 5(b) shows that a weak columnlike structure along the polarization axis is developed. However, at $t = 14.99$ fs, the ionization is almost homogeneous except for the surface [Fig. 5(c)]. A completely different pattern is observed when the collisional ionization is turned off [Fig. 5(d)]. Figures 5(e) and 5(f) show the time evolution of the field E_y along the polarization axis for the case with and without collisional ionization, respectively. The internal field

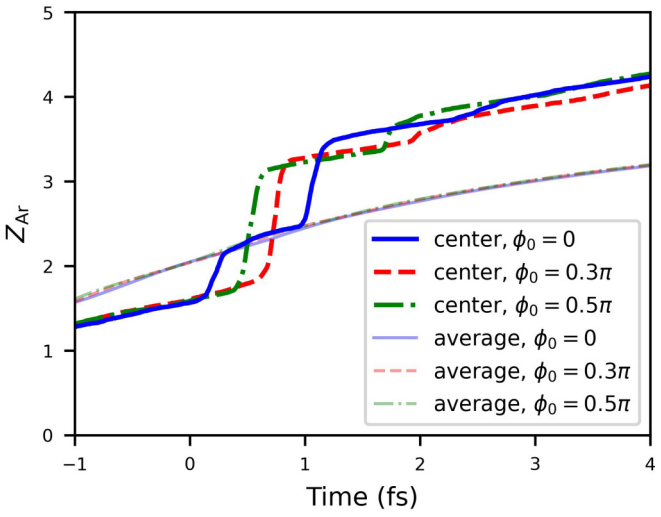

FIG. 6. Time evolution of the charge state at the center of the cluster and the charge state averaged over the entire cluster for three different carrier-envelope phases: 0, 0.3π, and 0.5π.

is weaker with the collisional ionization, leaving the cluster core less ionized.

As this ionization mechanism stems from the subcycle dynamics of the Brunel electrons and works best with few-cycle pulses, the role of the carrier-envelope phase deserves attention. Figure 6 shows the variations of the charge state at the cluster center and the volume-averaged charge state for three different carrier-envelope phases. The solid blue curves (both in bright color and in muted color) represent the results from the same simulation as in Fig. 1, where $\phi_0 = 0$ is used. The dashed red curves and dash-dotted green curves represent the cases with $\phi_0 = 0.3\pi$ and $\phi_0 = 0.5\pi$, respectively. The subcycle evolution of the charge state at the cluster center is quite different, but the final charge state at the center, which is a time-integrated effect, shows little variation with the carrier-envelope phase. The volume-averaged charge state is almost identical for the three cases at all the times.

In addition to the pulse duration and carrier-envelope phase, we also investigate other configurations. Figures 7(a) and 7(b) show the snapshot of the charge state distribution at $t = 10.02$ fs for 30-nm- and 50-nm-sized clusters. The pattern is similar, although a larger size produces a slightly lower maximum charge state at the center. This mechanism is necessarily associated with the curvature of the cluster surface. For a phantom cubic cluster as shown in Fig. 7(c), no core ionization is observed. Without the focusing of the wave due to the spherical geometry, the field is not strong enough to create appreciable ionization. Figure 7(d) shows the case with a much higher intensity of 5×10^{17} W/cm^2. Due to the big gap of the ionization potential for Ar^{8+}, the ionization is saturated to some degree, leading to a smaller anisotropy.

Our mechanism shares two steps of the semiclassical three-step model of high-order-harmonic generation for atoms [27], which are the ionization and propagation. However, the last step of the three-step model is an electron-impact process, while our scenario relies on the field from the Brunel-electron-driven plasma oscillation. If the Brunel electrons are

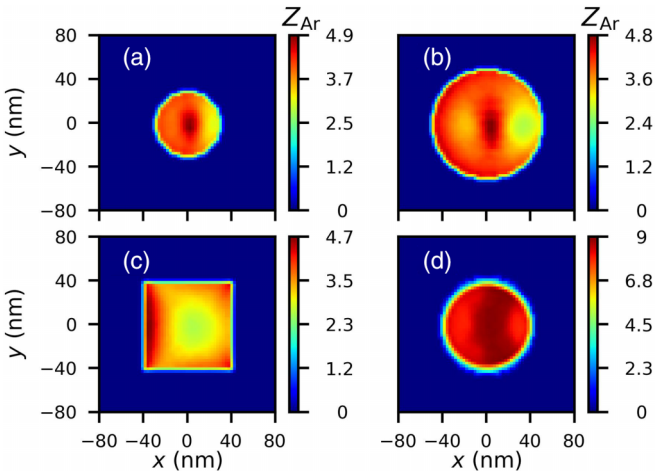

FIG. 7. Charge state distribution in the y-x plane at $t = 10.02$ fs for (a) a spherical cluster of 30 nm radius, (b) a spherical cluster of 50 nm radius, (c) a phantom cubic cluster of 80 nm, (d) a 40-nm cluster with an intensity of 5×10^{17} W/cm^2. Other unspecified parameters are the same as in Fig. 1.

considered as one macroparticle and the clustered plasma is considered as another macroparticle, our mechanism could be described as a globally "three-step-like" model. This ionization mechanism could perhaps be inferred from other observations, but has not received attention before probably due to the following reasons. First, quite a few studies consider micrometer-sized hydrogen clusters or helium droplets [28,29]. As the core of these large clusters remains un-ionized, the plasma-wave-driven ionization is absent. Second, this effect manifests itself in the few-cycle regime, which is less explored because the majority of terawatt laser systems generate pulses of several tens of femtoseconds duration. Third, the study of laser-cluster interaction is heavily motivated by the application of energetic particle generation, where an ultraintense laser pulse with an intensity exceeding 10^{17} W/cm^2 is often used. At such an intensity, the ionization is complete at the leading edge of the pulse, and the ionization dynamics is not of particular interest.

Our scenario bears some similarities with previously studied attosecond plasma wave dynamics in nanoplasmas [30]. However, resonant conditions were required in the scheme in Ref. [30], which were met by using a pump-probe scheme. The resonant excitation caused a field enhancement of several orders of magnitude and altered the dynamics of collisional ionization, allowing a strongly nonuniform ion charge distribution at longer pulse duration. An ionization hot spot at the cluster core was also demonstrated for a helium nanodroplet doped with a tiny xenon cluster [31]. Recently, it was found that clusters pumped with a longer wavelength produce a columnlike inhomogeneous charge distribution. However, cluster poles remain the preferred sites for ionization [18].

IV. CONCLUSION

In summary, we have identified an ionization mechanism for nanoclusters in intense ultrashort laser pulses using particle-in-cell simulations. In a partially ionized cluster, the returning Brunel electrons form an attosecond bunch and drive plasma oscillation impulsively. The resulting electric field causes higher ionization. This scheme is favored at shorter pulse duration, where collisional ionization plays a minor role. With the increasing availability of intense few-cycle laser sources and the advancement of single-shot coherent x-ray diffractive imaging techniques [32,33], it is feasible to test this anisotropic ionization experimentally. Our study will stimulate further experimental investigation and may offer a convenient way to control the ionization and heating in nanometer-sized targets by using few-cycle pulses with an engineered curvature of the target surface.

ACKNOWLEDGMENTS

This work was supported by the Natural Science Foundation of Zhejiang Province (Grant No. LY19A040005).

[1] V. P. Krainov and M. B. Smirnov, Cluster beams in the superintense femtosecond laser pulse, Phys. Rep. **370**, 237 (2002).
[2] T. Fennel, K. H. Meiwes-Broer, J. Tiggesbäumker, P. G. Reinhard, P. M. Dinh, and E. Suraud, Laser-driven nonlinear cluster dynamics, Rev. Mod. Phys. **82**, 1793 (2010).
[3] K. K. Ostrikov, F. Beg, and A. Ng, Nanoplasmas generated by intense radiation, Rev. Mod. Phys. **88**, 011001 (2016).
[4] Y. Fukuda, A. Y. Faenov, M. Tampo, T. A. Pikuz, T. Nakamura, M. Kando, Y. Hayashi, A. Yogo, H. Sakaki, T. Kameshima, A. S. Pirozhkov, K. Ogura, M. Mori, T. Z. Esirkepov, J. Koga, A. S. Boldarev, V. A. Gasilov, A. I. Magunov, T. Yamauchi, R. Kodama *et al.*, Energy Increase in Multi-MeV Ion Acceleration in the Interaction of a Short Pulse Laser with a Cluster-Gas Target, Phys. Rev. Lett. **103**, 165002 (2009).
[5] R. Matsui, Y. Fukuda, and Y. Kishimoto, Quasimonoenergetic Proton Bunch Acceleration Driven by Hemispherically Converging Collisionless Shock in a Hydrogen Cluster Coupled with Relativistically Induced Transparency, Phys. Rev. Lett. **122**, 014804 (2019).
[6] T. Ditmire, J. Zweiback, V. P. Yanovsky, T. E. Cowan, G. Hays, and K. B. Wharton, Nuclear fusion from explosions of femtosecond laser-heated deuterium clusters, Nature (London) **398**, 489 (1999).
[7] J. Feng, W. Wang, C. Fu, L. Chen, J. Tan, Y. Li, J. Wang, Y. Li, G. Zhang, Y. Ma, and J. Zhang, Femtosecond Pumping of Nuclear Isomeric States by the Coulomb Collision of Ions with Quivering Electrons, Phys. Rev. Lett. **128**, 052501 (2022).
[8] H. M. Milchberg, S. J. McNaught, and E. Parra, Plasma hydrodynamics of the intense laser-cluster interaction, Phys. Rev. E **64**, 056402 (2001).
[9] L. Köller, M. Schumacher, J. Köhn, S. Teuber, J. Tiggesbäumker, and K. H. Meiwes-Broer, Plasmon-Enhanced Multi-Ionization of Small Metal Clusters in Strong Femtosecond Laser Fields, Phys. Rev. Lett. **82**, 3783 (1999).
[10] C. Jungreuthmayer, M. Geissler, J. Zanghellini, and T. Brabec, Microscopic Analysis of Large-Cluster Explosion in Intense Laser Fields, Phys. Rev. Lett. **92**, 133401 (2004).

[11] J. Psikal, O. Klimo, and J. Limpouch, Field ionization effects on ion acceleration in laser-irradiated clusters, Nucl. Instrum. Methods Phys. Res., Sect. A **653**, 109 (2011).

[12] A. M. Bystrov and V. B. Gildenburg, Infrared to Ultraviolet Light Conversion in Laser-Cluster Interactions, Phys. Rev. Lett. **103**, 083401 (2009).

[13] X. Gao, B. Shim, and M. C. Downer, Brunel harmonics generated from ionizing clusters by few-cycle laser pulses, Opt. Lett. **44**, 779 (2019).

[14] M. McCormick, A. V. Arefiev, H. J. Quevedo, R. D. Bengtson, and T. Ditmire, Observation of Self-Sustaining Relativistic Ionization Wave Launched by a Sheath Field, Phys. Rev. Lett. **112**, 045002 (2014).

[15] T. Ditmire, T. Donnelly, A. M. Rubenchik, R. W. Falcone, and M. D. Perry, Interaction of intense laser pulses with atomic clusters, Phys. Rev. A **53**, 3379 (1996).

[16] C. Fourment, B. Chimier, F. Deneuville, D. Descamps, F. Dorchies, G. Duchateau, M.-C. Nadeau, and S. Petit, Ultrafast changes in optical properties of SiO_2 excited by femtosecond laser at the damage threshold and above, Phys. Rev. B **98**, 155110 (2018).

[17] U. Saalmann, C. Siedschlag, and J. M. Rost, Mechanisms of cluster ionization in strong laser pulses, J. Phys. B **39**, R39 (2006).

[18] H. Park, A. Camacho Garibay, Z. Wang, T. Gorman, P. Agostini, and L. F. DiMauro, Unveiling the Inhomogeneous Nature of Strong Field Ionization in Extended Systems, Phys. Rev. Lett. **129**, 203202 (2022).

[19] T. Taguchi, T. M. Antonsen, and H. M. Milchberg, Resonant Heating of a Cluster Plasma by Intense Laser Light, Phys. Rev. Lett. **92**, 205003 (2004).

[20] B. N. Breizman, A. V. Arefiev, and M. V. Fomyts'kyi, Nonlinear physics of laser-irradiated microclusters, Phys. Plasmas **12**, 056706 (2005).

[21] F. Brunel, Not-So-Resonant, Resonant Absorption, Phys. Rev. Lett. **59**, 52 (1987).

[22] F. Quere, C. Thaury, P. Monot, S. Dobosz, P. Martin, J. P. Geindre, and P. Audebert, Coherent Wake Emission of High-Order Harmonics from Overdense Plasmas, Phys. Rev. Lett. **96**, 125004 (2006).

[23] C. Thaury and F. Quéré, High-order harmonic and attosecond pulse generation on plasma mirrors: basic mechanisms, J. Phys. B: At., Mol. Opt. Phys. **43**, 213001 (2010).

[24] J. Derouillat, A. Beck, F. Pérez, T. Vinci, M. Chiaramello, A. Grassi, M. Flé, G. Bouchard, I. Plotnikov, N. Aunai, J. Dargent, C. Riconda, and M. Grech, SMILEI: A collaborative, open-source, multi-purpose particle-in-cell code for plasma simulation, Comput. Phys. Commun. **222**, 351 (2018).

[25] X. Gao, Ionization dynamics of sub-micrometer-sized clusters in intense ultrafast laser pulses, Phys. Plasmas **30**, 052102 (2023).

[26] X. Gao, A. V. Arefiev, R. C. Korzekwa, X. Wang, B. Shim, and M. C. Downer, Spatio-temporal profiling of cluster mass fraction in a pulsed supersonic gas jet by frequency-domain holography, J. Appl. Phys. **114**, 034903 (2013).

[27] P. B. Corkum, Plasma perspective on strong field multiphoton ionization, Phys. Rev. Lett. **71**, 1994 (1993).

[28] T. V. Liseykina and D. Bauer, Plasma-Formation Dynamics in Intense Laser-Droplet Interaction, Phys. Rev. Lett. **110**, 145003 (2013).

[29] U. Zastrau, P. Sperling, C. Fortmann-Grote, A. Becker, T. Bornath, R. Bredow, T. Döppner, T. Fennel, L. B. Fletcher, E. Förster, S. Göde, G. Gregori, M. Harmand, V. Hilbert, T. Laarmann, H. J. Lee, T. Ma, K. H. Meiwes-Broer, J. P. Mithen, C. D. Murphy *et al.*, Ultrafast electron kinetics in short pulse laser-driven dense hydrogen, J. Phys. B: At., Mol. Opt. Phys. **48**, 224004 (2015).

[30] C. Varin, C. Peltz, T. Brabec, and T. Fennel, Attosecond Plasma Wave Dynamics in Laser-Driven Cluster Nanoplasmas, Phys. Rev. Lett. **108**, 175007 (2012).

[31] A. Mikaberidze, U. Saalmann, and J. M. Rost, Laser-Driven Nanoplasmas in Doped Helium Droplets: Local Ignition and Anisotropic Growth, Phys. Rev. Lett. **102**, 128102 (2009).

[32] T. Gorkhover, S. Schorb, R. Coffee, M. Adolph, L. Foucar, D. Rupp, A. Aquila, J. D. Bozek, S. W. Epp, B. Erk, L. Gumprecht, L. Holmegaard, A. Hartmann, R. Hartmann, G. Hauser, P. Holl, A. Hömke, P. Johnsson, N. Kimmel, K.-U. Kühnel *et al.*, Femtosecond and nanometre visualization of structural dynamics in superheated nanoparticles, Nat. Photonics **10**, 93 (2016).

[33] C. Bacellar, A. S. Chatterley, F. Lackner, C. D. Pemmaraju, R. M. P. Tanyag, D. Verma, C. Bernando, S. M. O. O'Connell, M. Bucher, K. R. Ferguson, T. Gorkhover, R. N. Coffee, G. Coslovich, D. Ray, T. Osipov, D. M. Neumark, C. Bostedt, A. F. Vilesov, and O. Gessner, Anisotropic Surface Broadening and Core Depletion during the Evolution of a Strong-Field Induced Nanoplasma, Phys. Rev. Lett. **129**, 073201 (2022).